

Table S1. System composition (waters and ions) used in simulations.

System	Water molecules (TIP3)	Na ⁺ ions (SOD)	Cl ⁻ ions (CLA)
APO	19080	67	54
PIY	23123	78	65
AND	19080	67	54
EST	18440	65	52
TES	19093	67	54

Table S2. Non-standard protonation states used in simulations.

Residue indices refer to the residue number (resnr) in the protein topology files (PROA_*.itp). Histidine tautomers were specified as HSD (δ -protonated; equivalent to HID). No other non-standard protonation states (e.g., HSE/HSP, ASH/GLH, LYP) were used.

System	Residue type	Non-standard state	Residue indices (resnr in PROA.itp)	Note
APO	His	HSD (δ -protonated; HID)	33, 47, 55, 103, 151, 158, 177, 248, 327, 343, 351	CHARMM-GUI/force-field assignment at pH 7.4
PIY	His	HSD (δ -protonated; HID)	33, 47, 55, 103, 151, 158, 177, 248, 327, 343, 351	CHARMM-GUI/force-field assignment at pH 7.4
AND	His	HSD (δ -protonated; HID)	33, 47, 55, 103, 151, 158, 177, 248, 327, 343, 351	CHARMM-GUI/force-field assignment at pH 7.4
EST	His	HSD (δ -protonated; HID)	33, 47, 55, 103, 151, 158, 177, 248, 327, 343, 351	CHARMM-GUI/force-field assignment at pH 7.4
TES	His	HSD (δ -protonated; HID)	33, 47, 55, 103, 151, 158, 177, 248, 327, 343, 351	CHARMM-GUI/force-field assignment at pH 7.4

Table S3. Docking pose quality check (YASARA; top two retained poses per ligand).

Notes: Docking score and dissociation constants are taken from YASARA docking logs (Bind.energy and K_d). Geometric plausibility metrics were computed from the exported PDB structures: min dist to Fe = minimum heavy-atom distance between ligand (UNL) and heme iron (HEM-Fe); min steric dist = minimum heavy-atom distance between ligand and receptor (protein + heme, excluding waters); clash is flagged when min steric dist < 2.0 Å; contact residues count unique protein residues with any heavy atom within 4.0 Å of ligand heavy atoms.

Ligand	Pose	Bind.energy (kcal/mol)	K_d (pM)	min dist to Fe (Å)	min steric dist (Å)	clash (<2.0 Å)	contact residues (≤ 4 Å)
EST	001	11.541	3470.0427	7.7747	3.1894	0	7
EST	002	11.541	3470.0427	9.9945	3.0403	0	4
AND	001	12.391	826.5641	8.0845	3.2426	0	6
AND	002	12.391	826.5641	10.2721	2.8661	0	6
TES	001	12.454	743.1851	7.7738	3.1950	0	6
TES	002	12.454	743.1851	10.4017	3.1373	0	6

Table S4. Docking score ranking for the three docked steroid ligands (AND, EST, and TES) from YASARA logs (top 10 runs per ligand).

Notes: PIY is not listed because the crystallographic PIY pose from PDB 3NC7 was used directly and was not subjected to redocking. Values were extracted directly from the YASARA docking log files. Bind.energy is reported by YASARA as the docking binding-energy score (kcal/mol). N_contact_residues refers to the contact count reported in the YASARA docking log and is not directly equivalent to the geometric contact count listed in Table S3.

Ligand	Run	Bind.energy (kcal/mol)	K_d (pM)	N_contact_residues (log)
AND	001	12.391	826.5641	1
AND	002	12.391	826.5641	1
AND	003	12.111	1325.9260	1
AND	004	12.111	1325.9260	1
AND	005	11.965	1696.4408	1
AND	006	11.965	1696.4408	1

AND	007	11.767	2369.5979	1
AND	008	11.767	2369.5979	1
AND	009	11.309	5133.2578	1
AND	010	11.309	5133.2578	1
EST	001	11.541	3470.0427	1
EST	002	11.541	3470.0427	1
EST	003	11.362	4694.0054	1
EST	004	11.362	4694.0054	1
EST	005	11.144	6781.7173	1
EST	006	11.144	6781.7173	1
EST	007	10.854	11064.0088	1
EST	008	10.854	11064.0088	1
EST	009	10.669	15118.8691	1
EST	010	10.669	15118.8691	1
TES	001	12.454	743.1851	1
TES	002	12.454	743.1851	1
TES	003	12.027	1527.8900	1
TES	004	12.027	1527.8900	1
TES	005	11.702	2644.3582	1
TES	006	11.702	2644.3582	1
TES	007	11.518	3607.3979	1
TES	008	11.518	3607.3979	1
TES	009	10.968	9127.4482	1
TES	010	10.968	9127.4482	1

Table S5. State fractions (%) and gating indices (CR, PI) on the $d_{\text{mouth}}/d_{\text{cover}}$ plane from 0–1000 ns using pooled (global) k-means centroids and nearest-centroid assignment. $CR = P_{\text{Closed}} / P_{\text{Open}}$; $PI = (P_{\text{Open}} + P_{\text{Closed}})/P_{\text{Intermediate}}$. Higher CR indicates closed enrichment; higher PI indicates intermediate depletion (end-state polarization).

System	Open	Intermediate	Closed	Closedness Ratio	Polarization Index
APO	4	95.8	0.1	0.03	0.04
PIY	4.9	95	0.1	0.02	0.05
AND	12.7	87.2	0.1	0.01	0.15
EST	97.7	1.9	0.4	<0.01	51.36
TES	26.7	29.5	43.8	1.64	2.39

Table S6. MSM-derived macrostate populations and kinetics (macrostates mapped by pooled Fig. 6 centroids).

System Open (%) Intermediate (%) Closed (%) MFPT (Closed → Open)

	System Open (%)	Intermediate (%)	Closed (%)	MFPT (Closed → Open)
APO	3.63	96.28	0.09	471.42
AND	11.92	88.05	0.03	168.98
EST	97.57	2.11	0.32	29.31
PIY	4.68	95.25	0.06	438.38
TES	27.11	29.39	43.50	326.67

Table S7. Transient ion proximity to the immediate catalytic region before MM-PBSA ion stripping

System	Sampled frames	Na ⁺ within 5 Å, n (%)	Cl ⁻ within 5 Å, n (%)	Max simultaneous Na ⁺	Max simultaneous Cl ⁻	Min Na ⁺ distance (Å)	Min Cl ⁻ distance (Å)
AND	1001	304 (30.37)	124 (12.39)	3	2	2.106	2.181
PIY	1001	254 (25.37)	132 (13.19)	4	2	2.170	2.166
EST	1001	285 (28.47)	209 (20.88)	3	2	2.194	2.081
TES	1001	212 (21.18)	186 (18.58)	3	2	2.072	2.025

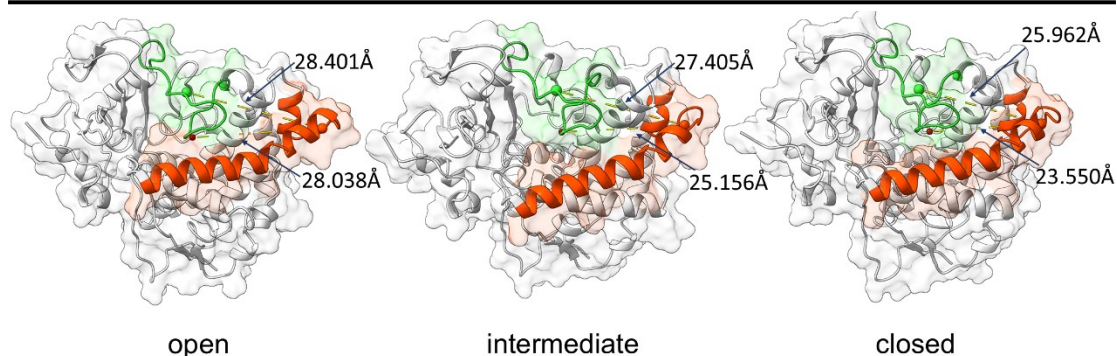


Figure S1. Apo CYP134A1 (CypX) open–intermediate–closed conformations highlighting mouth–cover gating.

Representative apo structures for the open, intermediate, and closed states are shown as a light-gray cartoon with a semi-transparent surface. The mouth (B'/C rim, residues 55–90) is colored orange and the FG cover (residues 173–209) is colored green. Distances (Å) report the mouth opening (C α centroid distance for 55–90) and the FG cover closure (FG-loop centroid, residues 198–203, to

heme Fe).

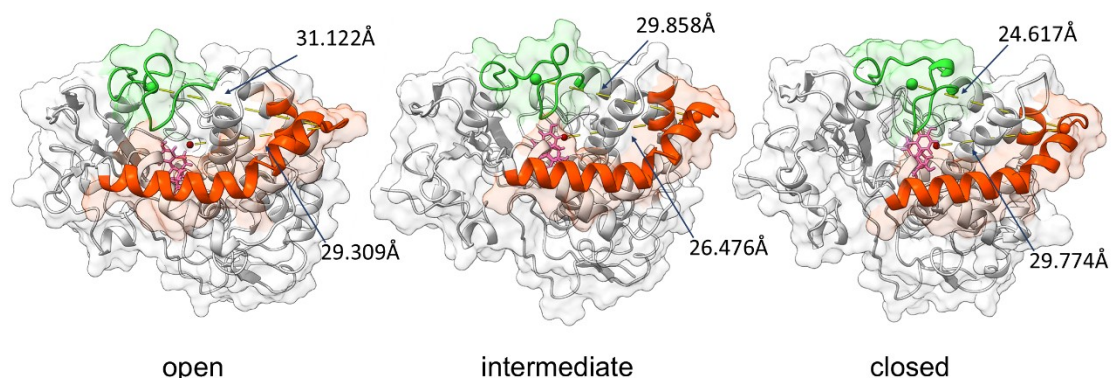


Figure S2. EST-bound CYP134A1 (CypX) open–intermediate–closed conformations highlighting mouth–cover gating.

Representative structures from the EST complex trajectory are shown for the open, intermediate, and closed states (light-gray cartoon with semi-transparent surface). The mouth (B'/C rim, residues 55–90) is colored orange and the FG cover (residues 173–209) is colored green; the EST ligand is shown as hotpink sticks. Distances (Å) report the mouth opening (Ca centroid distance for residues 55–90) and FG cover closure (FG-loop centroid, residues 198–203, to heme Fe).

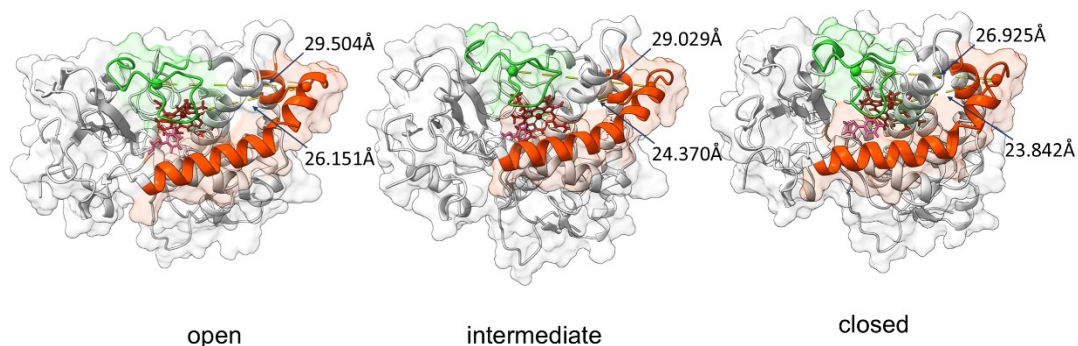


Figure S3. PIY-bound CYP134A1 (CypX) open–intermediate–closed conformations highlighting mouth–cover gating.

Representative structures from the PIY complex trajectory are shown for the open, intermediate, and closed states (light-gray cartoon with semi-transparent surface). The mouth (B'/C rim, residues 55–90) is colored orange and the FG cover (residues 173–209) is colored green; the PIY ligand is shown as hotpink sticks. Distances (Å) report the mouth opening (Ca centroid distance for

residues 55–90) and FG cover closure (FG-loop centroid, residues 198–203, to heme Fe).

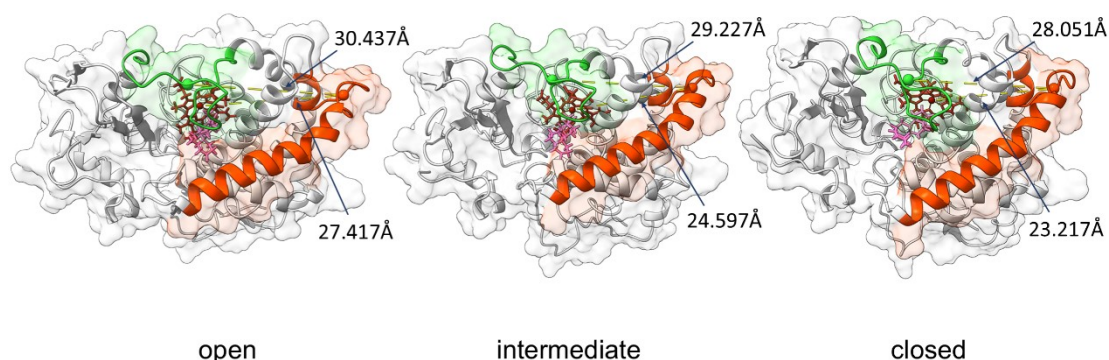


Figure S4. AND-bound CYP134A1 (CypX) open–intermediate–closed conformations highlighting mouth–cover gating.

Representative structures from the AND complex trajectory are shown for the open, intermediate, and closed states (light-gray cartoon with semi-transparent surface). The mouth (B'/C rim, residues 55–90) is colored orange and the FG cover (residues 173–209) is colored green; the AND ligand is shown as hotpink sticks. Distances (Å) report the mouth opening (Ca centroid distance for residues 55–90) and FG cover closure (FG-loop centroid, residues 198–203, to heme Fe).

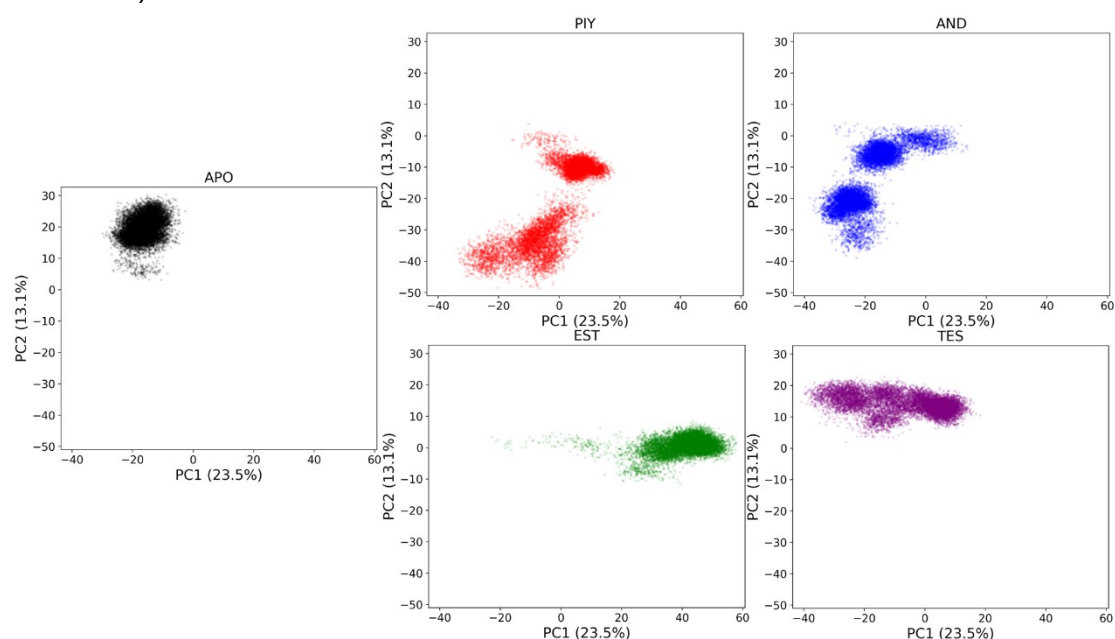


Figure S5. System-separated PCA distributions for the five simulated CypX ensembles.

Principal component analysis (PCA) projections of the pooled trajectories are shown separately for the APO, PIY, AND, EST, and TES systems in the PC1–PC2 space. Each point represents one sampled frame projected onto the first two principal components, using the same eigenvector basis and the same axis ranges as in the combined PCA plot shown in the main text. Colors are consistent with the main figures: APO, black; PIY, red; AND, blue; EST, green; TES, purple. These system-separated plots were included to facilitate clearer inspection of the conformational distributions sampled by each individual ensemble.